Int. J. Heat Mass Transfer, Vol. 25, No. 1, pp. 77–86, 1982.
Printed in Great Britain

0017-9310/82/010077-10 $03.00/0
Pergamon Press Ltd.

THE EMPIRICAL DESCRIPTION OF TURBULENT CHANNEL FLOWS

M. M. M. EL TELBANY* and A. J. REYNOLDS
Department of Mechanical Engineering, Brunel University, Uxbridge, Middlesex, U.K.

(*Received* 3 *February* 1981 *and in revised form* 3 *April* 1981)

Abstract—Measurements made in 26 asymmetric turbulent channel flows (that is, flows in a broad channel, typically with unequal stresses at the two walls) are presented in the form of mixing lengths and eddy viscosities. Ranges of applicability of simple empirical formulae are defined and friction laws for the wall stresses are developed.

NOMENCLATURE

b, channel breadth;
C, E, constants in gradient law;
C_f, $= 2\tau_1/\rho U_a^2$, friction coefficient;
D, constant;
G_1, constant in equation for friction coefficient;
h, channel half-depth;
K, von Kàrmàn's constant;
l, mixing length;
P, mean static pressure;
Re_a, $= 2hU_a/\nu$, Reynolds number based on average velocity and channel depth;
Re_b, $= 2hU_b/\nu$, Reynolds number based on belt velocity and channel depth;
Re_m, $= 2hU_m/\nu$, Reynolds number based on maximum velocity and channel depth;
U, time-averaged velocity component in x-direction;
U_a, average velocity;
U_b, belt velocity;
U_m, maximum velocity;
u_*, $= \sqrt{(\tau_w/\rho)}$, friction velocity based on wall stress;
u_{*e}, $= \sqrt{[(|\tau_1| + |\tau_2|)/\rho]}$, effective friction velocity;
$\dot{V}$, flow rate;
x, co-ordinate in the direction of main flow;
y, normal distance measured from one wall.

Greek symbols

τ, shear stress;
γ, $= \tau_2/\tau_1$, ratio of the shear stresses at the walls;
ρ, fluid density;
ν, fluid kinematic viscosity;
α, local gradient of the kinematic shear stress;
ε, eddy viscosity.

Subscripts

1, denotes high-stress wall;
2, denotes low-stress wall;
m, refers to maximum velocity;
0, refers to zero turbulent shear stress;
w, denotes wall.

* Permanent address: Faculty of Engineering, Helwan University, Elmataria, Cairo, Egypt.

1. INTRODUCTION

IN OTHER papers [1–4] the present authors have presented measurements made in 26 flows in a channel, one of whose walls is a moving belt. The channel is sufficiently broad (aspect ratio typically $b/2h = 18$) and sufficiently long (development distance typically $x/2h = 30$, following a turbulence-inducing mesh) to generate a reasonable approximation to fully developed plane turbulent flow. In addition to the cases of plane Poiseuille and plane Couette flow, which have been given some attention in the past, 19 intermediate motions were studied. These can be separated into two classes:

(a) Poiseuille-type flows, with a maximum mean velocity within the turbulent flow, and wall-stress ratio $\tau_2/\tau_1 < 0$; and

(b) Couette-type flows, with the mean velocity varying monotonically across the channel to a maximum at the moving wall, and wall-stress ratio $\tau_2/\tau_1 > 0$.

These investigations provide the first comprehensive body of empirical information relating to the often discussed case of plane channel flow with unequal wall stresses, although there have been some studies of flows in channels with differing wall roughness [5], and a study of developing flow in a channel with a moving wall was carried out as long ago as 1914 [6].

Situations which give rise to fluid motions of the general character of those considered here occur commonly in engineering practice. In particular we may mention: turbulent lubrication films, smooth- and rough-walled annuli, plane channels with differing wall roughness as are sometimes found in heat exchangers, and passages between the rotors and fixed elements of rotating machinery such as pumps, turbines and electric motors. Typically, the heat transfer associated with these motions is of equal or greater interest than are the fluid motions themselves. To assist

Table 1. Details of tests

Case	$2h$ (mm)	U_b (ms^{-1})	U_m (ms^{-1})	U_a (ms^{-1})	$\frac{Re_a}{1000}$	$\frac{Re_b}{1000}$	$\frac{Re_m}{1000}$	u_{*1} (ms^{-1})	u_{*2} (ms^{-1})	γ	$\frac{y_0}{h}$	$\frac{y_m}{h}$
1	66	12.84	12.84	6.42	28.50	57.01	57.01	0.282	0.282	1.000	—	—
2	66	12.84	12.84	7.28	32.33	57.01	57.01	0.328	0.233	0.504	—	—
3	66	12.84	12.84	8.06	35.80	57.01	57.01	0.362	0.1809	0.250	—	—
4	66	12.84	12.84	8.14	36.14	57.01	57.01	0.357	0.1667	0.217	—	—
5	66	12.84	12.84	8.81	39.11	57.01	57.01	0.383	0.1305	0.116	—	—
6	66	8.59	8.59	6.71	29.79	38.14	38.14	0.313	0.0615	0.0386	—	—
7	101	17.08	17.08	14.55	98.80	116.05	116.05	0.600	0.0400	0.0044	—	—
8	101	12.84	12.84	11.38	77.30	87.24	87.24	0.485	0.0229	0.00223	—	—
9	101	8.59	8.59	7.79	52.94	58.36	58.36	0.350	0.0084	0.00057	—	—
10	66	12.84	13.25	12.40	55.07	57.01	58.83	0.564	0.0300	−0.0028	1.994	1.55
11	66	12.84	16.33	15.10	67.05	57.01	72.51	0.679	0.1860	−0.075	1.860	1.44
12	66	12.84	21.57	20.11	89.28	57.01	95.77	0.880	0.4142	−0.2215	1.637	1.22
13	66	12.84	24.01	22.40	99.48	57.01	106.61	0.978	0.518	−0.2805	1.560	1.20
14	66	8.59	23.62	21.90	97.25	38.14	104.86	0.961	0.670	−0.485	1.347	1.10
15	66	—	16.00	14.55	64.60	—	71.04	0.659	0.659	−1.000	1.000	1.00
16	44	12.84	12.84	6.42	19.00	38.00	38.00	0.293	0.293	1.000	—	—
17	44	17.08	17.08	8.54	25.28	50.56	50.56	0.378	0.378	1.000	—	—
18	66	17.08	17.08	8.54	37.92	75.83	75.83	0.363	0.363	1.000	—	—
19	66	12.84	12.84	6.72	29.83	57.01	57.01	0.303	0.267	0.775	—	—
20	66	12.84	12.84	9.53	42.32	57.01	57.01	0.431	0.1089	0.0635	—	—
21	66	12.84	12.84	9.67	42.92	57.01	57.01	0.435	0.1035	0.0566	—	—
22	66	12.84	18.27	16.89	75.02	57.01	81.12	0.740	0.269	−0.132	1.767	1.34
23	66	8.59	13.81	12.87	57.13	38.14	61.32	0.600	0.256	−0.1816	1.693	1.26
24	66	8.59	15.05	14.02	62.24	38.14	66.82	0.645	0.306	−0.225	1.633	1.22
25	44	—	25.80	23.52	69.62	—	76.37	1.040	1.040	−1.000	1.000	1.00
26	66	—	12.60	11.42	50.70	—	55.95	0.514	0.514	−1.000	1.000	1.00

y_0 and y_m measured from high-stress wall.

in the application of our work to such situations, we shall in the present paper recast our results in terms of the semi-empirical devices commonly used in engineering calculations: mixing lengths, eddy viscosities, and wall-friction coefficients.

These formulations are of particular use and interest when they correlate the data describing a number of channel flows of the class considered here, and it is on such widely applicable results that we shall concentrate.

2. BASIC RESULTS

Table 1 lists the leading features of the flows studied, and includes the three Reynolds numbers characterizing each flow. These are based, respectively, on belt speed U_b, maximum time-mean velocity U_m (equal to U_b for Couette-type flows), and the average velocity U_a obtained by averaging across the channel section. In each case one or more of these Reynolds numbers lies in the range 40,000 to 120,000, and there can be no doubt that the results exhibit the characteristics of well established turbulent motion. The Reynolds number which we shall find most convenient in characterizing this class of motions is Re_a, that based on the average velocity U_a. (Note that U_b vanishes in the important limiting case of Poiseuille flow, and that for Poiseuille-type flows U_m cannot be deduced prior to an experiment nor in typical applications.)

Also given in Table 1 are the friction velocities u_{*1} and u_{*2}† corresponding to the usually differing wall stresses generated in each flow, and the ratio of the two wall stresses $\gamma = \tau_2/\tau_1$. We have adopted the convention that the subscript 1 labels the wall where the stress is larger. Thus $|\gamma| < 1$ in every case, while $\gamma = 1$ for pure shear (Couette) flow, and $\gamma = -1$ for pure pressure (Poiseuille) flow.

For Poiseuille-type flows a plane of maximum velocity and a plane of vanishing shear stress (in general, not coincident) appear within the channel, and their positions are indicated in Table 1. Figure 1 illustrates the main kinematic features of this class of flows and identifies several of the quantities appearing in the table.

† For more details see Appendix.

Figure 2 presents the ratio U_b/U_a of belt speed to average fluid velocity, as a function of the stress ratio γ. This empirical curve, which was not known to us until the experiments had been carried out, is the key to the design of further experiments of this type, for it specifies the stress ratio (which defines the particular flow which an experimenter wishes to examine, but it not under his immediate control) as a function of two parameters that are controllable, namely, the flow through the channel (very nearly $\dot{V} = 2U_s bh$) and the belt speed U_b. Moreover, as we shall see shortly, the correlation of Fig. 2 provides a convenient link between the controllable quantities (U_a and U_b) and the friction generated at the two walls, which one often seeks to predict in practical applications.

We have elsewhere [1] indicated the parts of these flows over which the ubiquitous logarithmic formula can be used to specify the mean-velocity variation, and formulae have been developed for the core region between the two, usually dissimilar wall layers.

3. FRICTION LAWS

If the friction at one wall is known, Fig. 2 allows us to determine that at the other wall once the flow-determining parameters (U_a and U_b) are specified. It remains to develop a method of predicting one of the wall stresses, or possibly their sum. While there undoubtedly exist a number of ways of presenting the friction measurements implicit in Table 1, the correlation of Fig. 2 is so successful that we have looked no further.

We consider the friction coefficient based on the larger stress and the average velocity:

$$c_f = \tau_1/(\tfrac{1}{2}\rho U_a^2) = 2(u_{*1}/U_a)^2 \qquad (1)$$

and postulate Reynolds number dependence of the form

$$(c_f/2)^{1/2} = u_{*1}/U_a = G_1/\log_{10} Re_a \,. \qquad (2)$$

This Reynolds number variation has been found to provide an adequate correlation of friction data for pipe flows, boundary layers and Couette flows, although a further empirical constant has sometimes been introduced, either by raising the logarithm to some power (as in the Prandtl–Schlichting pipe-friction formula) or by adding a constant to the

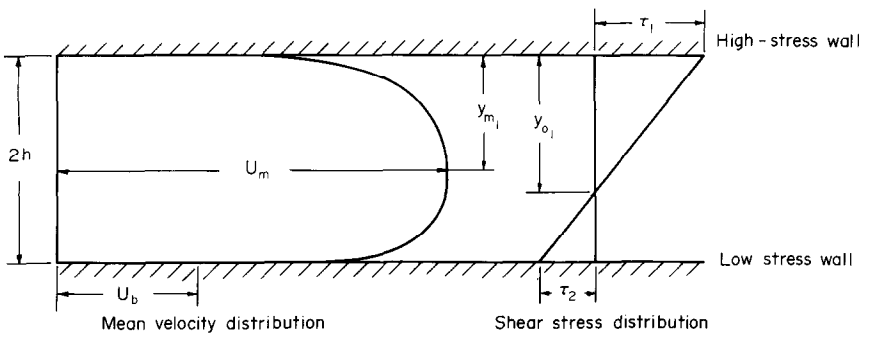

FIG. 1. Main kinematic features of the flow.

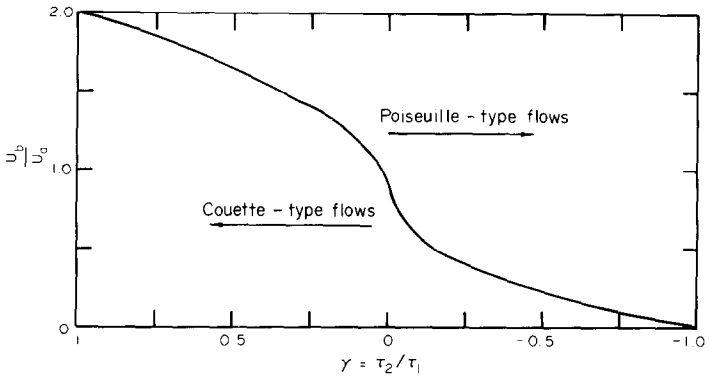

FIG. 2. Ratio of belt velocity to average velocity as a function of stress ratio.

logarithm (as in Squire and Young's boundary layer friction formula).

We must expect the parameter G_1 to be dependent on flow type, in other words, that it may be a function of the stress ratio γ. This functional dependence, if any, can be calculated from $G_1 = (u_{*1}/U_a)\log_{10} Re_a = (c_f/2)^{1/2}\log_{10} Re_a$. The results presented in Fig. 3 reveal that the variation in G_1 is little more than 10% over the entire range of γ, and some part of this variability may be attributed to experimental scatter. For $\gamma < 0$, we cannot do better than adopt the mean value:

$$G_1 = 0.2175 \text{ for Poiseuille-type flows,} \quad (3)$$

while for $\gamma > 0$ there is a modest dependence on flow species:

$$G_1 = 0.2105 - 0.015\gamma^{1.2} \text{ for Couette-type flows.} \quad (4)$$

The departures of the experimental values from these formulae are at most 2%. In equations (3) and (4) there is a discrepancy of some 3% in the values $\gamma(0+)$ and $\gamma(0-)$, but this mirrors faithfully the experimental results.

There is no reason to modify the Reynolds number dependence proposed in equation (2); note that while Re_a varies from 19,000 to 38,000 for the four Couette flows studied, the values of G_1 are virtually indistinguishable.

With the stress at one wall linked to the defining parameters as indicated above, the other stress follows from $\tau_2 = \gamma\tau_1$, with $\gamma = f(U_b/U_a)$ from Fig. 2. The pressure gradient can be found from

$$dp/dx = (\tau_1 - \tau_2)/2h = \tau_1(1-\gamma)/2h. \quad (5)$$

4. MIXING LENGTHS

We shall make use of two definitions of the mixing length, based respectively on the local shear stress at some distance from the wall and on the stress at the closer wall:

$$\left.\begin{aligned} l &= \frac{(\tau/\rho)^{1/2}}{dU/dy} \\ \text{and} \\ l_w &= \frac{(\tau_w/\rho)^{1/2}}{dU/dy} \end{aligned}\right\} \quad (6)$$

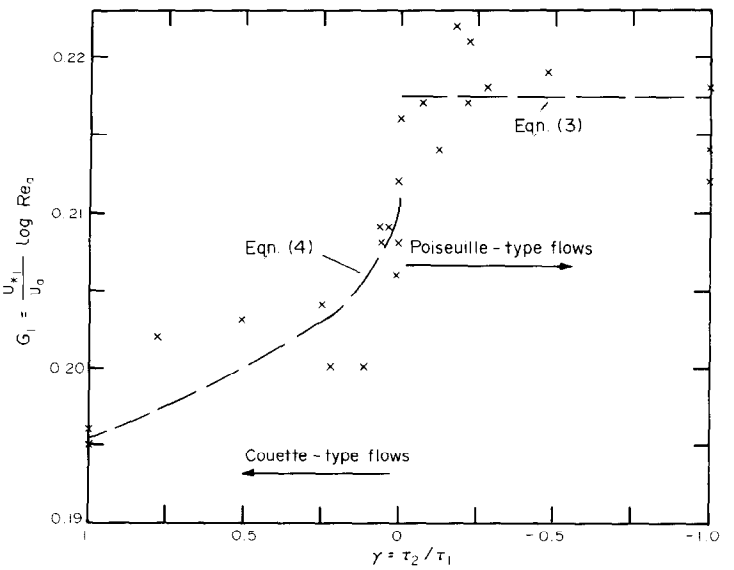

FIG. 3. Variation of G_1 with stress ratio. Dashed lines represent empirical formulae.

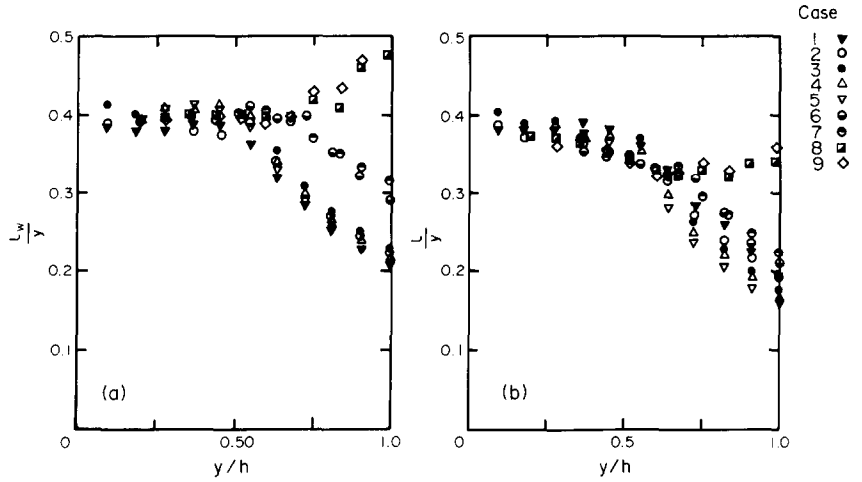

FIG. 4. Mixing-length distribution for the high-stress wall of Couette-type flows (y measured from high-stress wall): (a) based on wall shear stress; (b) based on local shear stress.

where

$$l_w = l(\tau_w/\tau)^{1/2}.$$

In these fully developed channel flows the two stresses are related by

$$\tau = \tau_w + \rho\alpha y. \tag{7}$$

where α is the (kinematic) stress gradient.

We are free to select whichever of the definitions (6) proves to give the more coherent representation of the data. Whichever is selected, it is expedient to present the results in the dimensionless form l/y or l_w/y, since these ratios may be expected to be equal to K, von Kàrmàn's constant, near a wall.

For Poiseuille-type flows we are also free to select whichever of the length scales h, y_m and y_0 proves to be the most effective in correlating the data. In fact, the scale y_0 is more useful than is y_m, since it is determined by

$$\frac{y_{01}}{h} = \frac{2}{1+|\gamma|} \quad \text{or} \quad \frac{y_{02}}{h} = \frac{2}{1+1/|\gamma|} \tag{8}$$

Figure 4 shows the variation of l_w/y and l/y vs y/h near the high-stress walls of Couette flows. In every case

$$l_w/y = 0.39 \quad \text{for} \quad y/h < 0.5 \tag{9a}$$

provides an adequate description. For low-stress walls in Couette-type flows (Fig. 5) such a simple prescription is not available. The best single formula is

$$l/y = 0.39 - 0.20\, y/h \quad \text{for } y/h < 1 \tag{9b}$$

but this is quite inadequate for cases where $\gamma = \tau_2/\tau_1 < 0.1$, and there is considerable scatter about this line even for flows with $\gamma > 0.1$.

Turning to Poiseuille-type motions, we see from Figs. 6 and 7 that

$$l_w/y = 0.39 \quad \text{for } y/y_{01} < 0.60 \tag{10a}$$

for all the flows near high-stress walls, and that

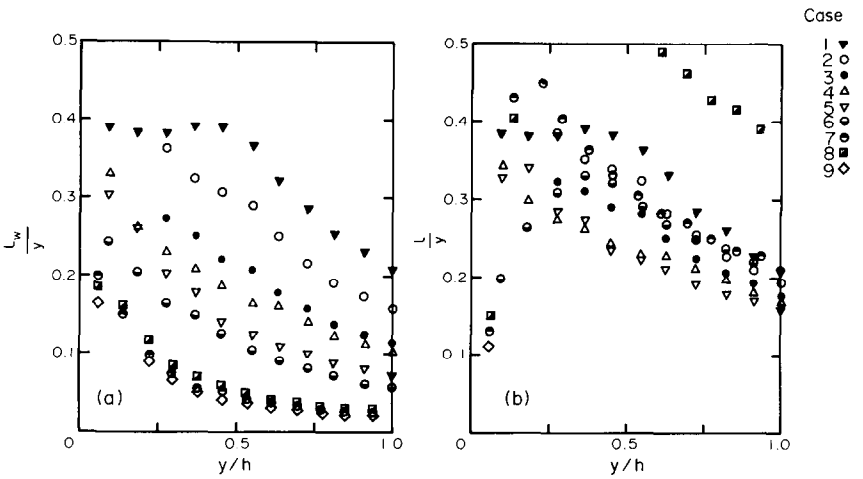

FIG. 5. Mixing-length distribution for the low-stress wall of Couette-type flows (y measured from low-stress wall): (a) based on wall shear stress; (b) based on local shear stress.

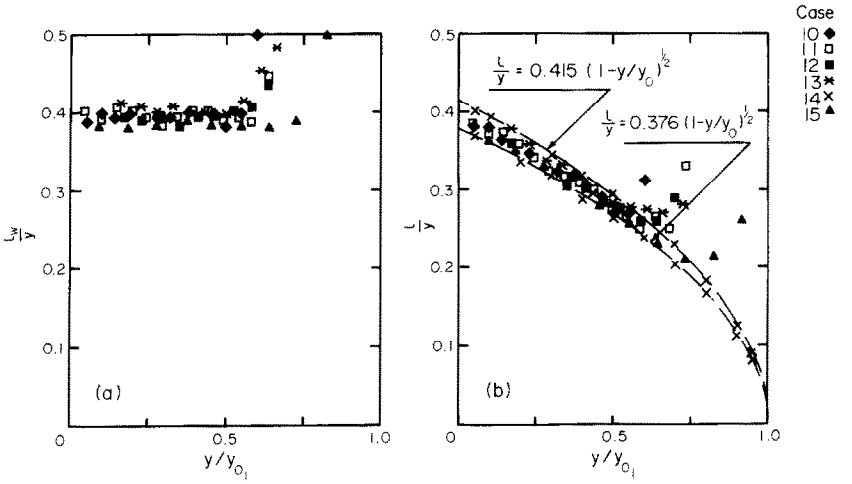

FIG. 6. Mixing-length distribution for the high-stress wall of Poiseuille-type flows (y and y_{01} measured from high-stress wall): (a) based on wall shear stress; (b) based on local shear stress.

$$l_w/y = 0.39 \quad \text{for } y/y_{02} < 0.80 \tag{10b}$$

for low-stress walls in flows where $|\gamma| > 0.1$.

Summarising, we note that simple mixing-length formulae are not applicable in the part of the flow adjacent to a wall at which the stress is less than one-tenth that at the high-stress wall. For a still wider range of Couette-type flows the motion adjacent to the low-stress wall fails to follow a simple pattern. However, some 70% of the cross-section of most Poiseuille-type flows can be accurately described by a simple mixing-length formula. Moreover, since the velocity gradients are comparatively small both in low-stress regions and in regions well away from the walls, a fair representation of the velocity variation can be obtained by assuming logarithmic velocity formulae to apply across the entire channel. This procedure will not define details such as planes of maximum velocity, nor will it usually define the transfer characteristics of the flow correctly.

5. EDDY VISCOSITIES

Again we consider definitions based on local and wall stresses:

$$\left.\begin{aligned} \varepsilon &= \frac{\tau/\rho}{\mathrm{d}U/\mathrm{d}y} = l(\tau/\rho)^{1/2} \\ \varepsilon_w &= \frac{\tau_w/\rho}{\mathrm{d}U/\mathrm{d}y} = l_w(\tau_w/\rho)^{1/2} \end{aligned}\right\} \tag{11}$$

where

$$\varepsilon_w = \varepsilon\tau_w/\tau.$$

As our interest here is primarily in the central part of the flow—the so-called core region between the wall layers—we adopt the channel half-width h as the length scale. Hence we consider variations of $\varepsilon/(u_* h)$ vs y/h. There is still some freedom in the choice of the

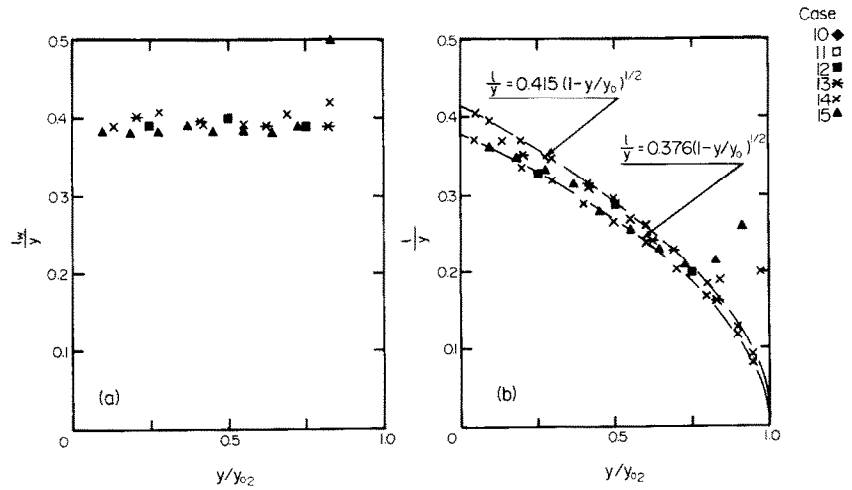

FIG. 7. Mixing-length distribution for the low-stress wall of Poiseuille-type flows (y and y_{02} measured from low-stress wall): (a) based on wall shear stress; (b) based on local shear stress.

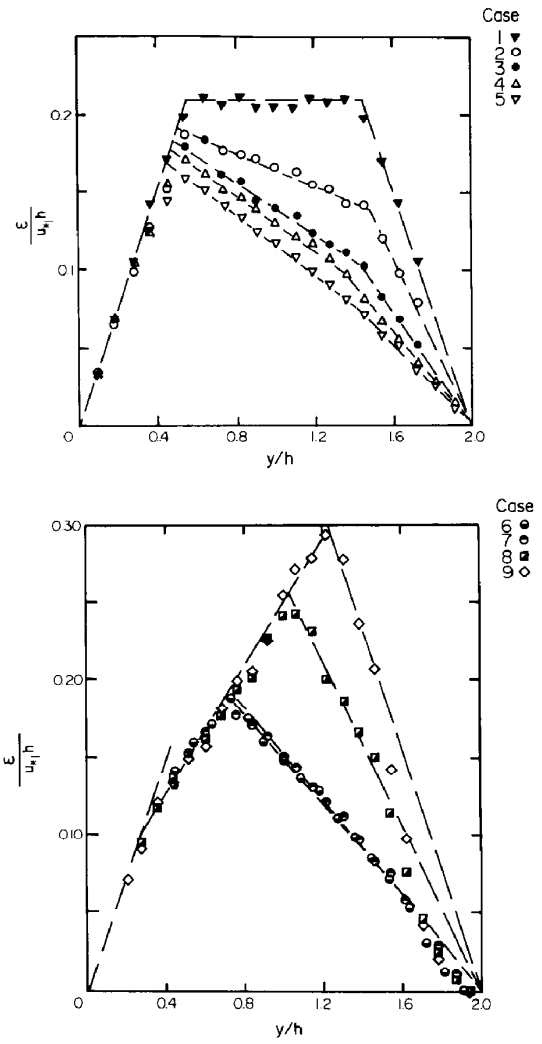

FIG. 8. Eddy viscosity distribution based on local shear stress for Couette-type flows (y measured from high-stress wall).

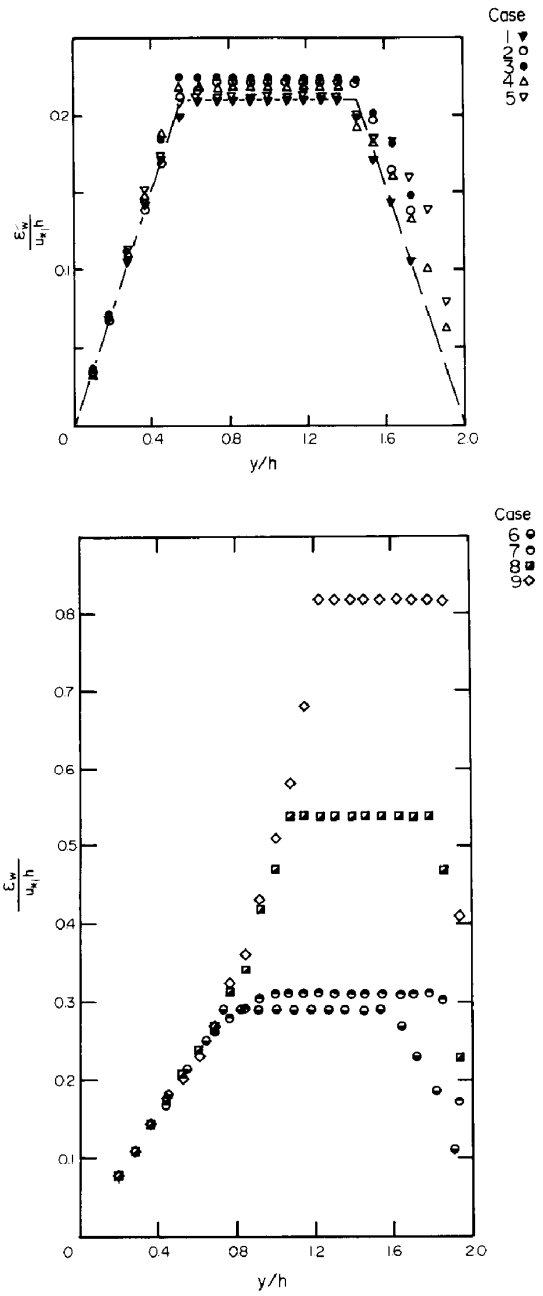

FIG. 9. Eddy viscosity distribution based on larger wall stress for Couette-type flows (y measured from high-stress wall).

scaling friction velocity u_*; this could be based on one of the wall stresses

$$\tau_1 = \rho u_{*1}^2 \tag{12a}$$

or

$$\tau_2 = \rho u_{*2}^2 \tag{12b}$$

or could be the 'effective' value given by

$$u_{*e}^2 = |\tau_1/\rho| + |\tau_2/\rho|. \tag{12c}$$

Figure 8 shows distributions of the conventional eddy viscosity ε based on local shear stress, for Couette-type flows. Since the eddy viscosity is fairly uniform in the core of pure Poiseuille flow ($\gamma = -1$) as well as in pure Couette flow ($\gamma = 1$), as shown here, it is somewhat surprising to find that for $0 < \gamma < 1$ there are very large (though nearly linear) variations within the central core. In [3] comparisons are made between the Poiseuille-flow results given here and those obtained earlier by Laufer [7] and Hussain and Reynolds [8]. Our results were found to be very close to the more recent measurements of Hussain and Reynolds.

Figure 9 reveals that the eddy viscosity ε_w based on the larger wall stress τ_1 presents a simpler pattern, with a nearly constant core value for any one flow, and that value nearly the same for all flows for which $\gamma > 0.1$:

$$\frac{\varepsilon_w}{u_{*1}\,h} = \frac{\tau_1/\rho}{\mathrm{d}U/\mathrm{d}y} = \frac{u_{*1}}{h\,\mathrm{d}U/\mathrm{d}y} = 0.215. \tag{13}$$

The collapse of the several eddy viscosity variations near the high stress wall is consistent with (and equivalent to) the mixing-length result (9a). Near the low-stress wall the situation cannot be described so

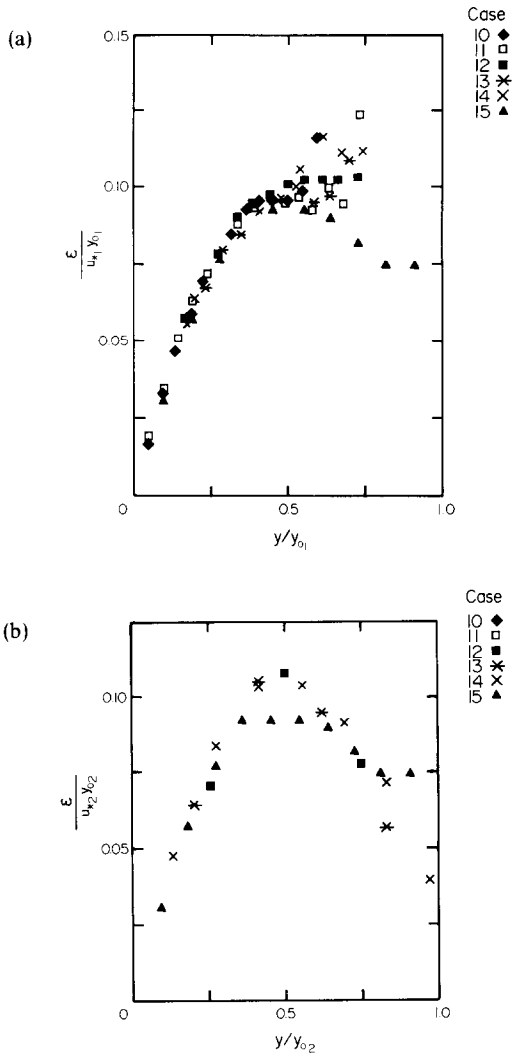

FIG. 10. Eddy viscosity distribution based on local shear stress for Poiseuille-type flows: (a) high-stress wall (y and y_{01} measured from high stress wall); (b) low-stress wall (y and y_{02} measured from low-stress wall).

easily, but we note that the region over which ε_w = constant extends very near to the low-stress wall as $\gamma \to 0$. Thus in this limit the higher stress τ_1 provides the appropriate scale for the eddy viscosity across almost the whole of the channel. It is plausible to suppose that this behaviour will arise also in an open-channel flow, where the stress at the free surface is a small fraction of that at the bottom.

The simple behaviour noted in Fig. 9 is consistent with the observation (reported in [1]) that the core velocities vary linearly for the entire class of Couette-type flows. Thus $h/(u_{*c}\, \mathrm{d}U/\mathrm{d}y) = D$, a constant, in the core of any one flow. Here u_{*c} is the effective value of the friction velocity defined in equation (12). There follows

$$\frac{\varepsilon_w}{u_{*1} h} = \frac{u_{*1}}{h\, \mathrm{d}U/\mathrm{d}y} = \frac{u_{*1}}{u_{*c} D} = \frac{1}{D(1 + |\gamma|)^{1/2}}.$$

In fact the constant $D \simeq 3.5$ for $\gamma > 0.005$, that is, for all the Couette flow cases save 8 and 9. Thus for Couette flow itself, $\varepsilon_w/(u_{*1} h) = 1/3.5\sqrt{2} = 0.2$, in close agreement with equation (13).

The concept of an eddy viscosity is less useful when applied to asymmetric ($\tau_1 \neq -\tau_2$) cases of the Poiseuille type. Unlike pure Poiseuille flow, these flows give rise to non-coincident planes of zero stress and maximum velocity. Hence $\varepsilon \to 0$ as $y \to y_0$ and $\varepsilon, \varepsilon_w \to \infty$ as $y \to y_m$. Thus any straightforward definition of eddy viscosity must give rise to large variations in the core region, pointing to the fundamental unreality of the gradient-diffusion hypothesis through which the eddy viscosity is introduced.

Figure 10 presents the eddy viscosity variations for Poiseuille-type flows in the most coherent manner which we have discovered and shows that scaling with the appropriate y_0 and u_* reduces the variations near the walls ($y/y_0 < 0.5$) to a standard pattern, though this fails to apply at the low-stress wall when $|\gamma| < 0.1$. This behaviour mirrors the mixing-layer results (10).

Although we shall not explore the matter in detail, it is worth noting that there is a marked difference between the eddy viscosity variation well away from the high-stress wall in the extreme cases 9 and 10, for which $\gamma = 0.00057$ and -0.0025, respectively. This observation suggests that the structure of the core turbulence is critically dependent on the sign of the vorticity generated at the low-stress wall, even if this is very small. In this connection we may note in Fig. 10(a) the 'collapse' of the core eddy viscosity in pure Poiseuille flow, where equal amounts of vorticity (but of opposite signs) are generated at the two walls.

One may ask how the transfer characteristics of the core of a Poiseuille-type flow are to be defined, for the purpose, say, of calculating the heat transfer from one wall to the other across a flow of this kind. Bearing in mind the linear distributions of Fig. 8 (admittedly arising in Couette-type flows) we propose that a linear variation of eddy diffusivity be adopted within the core of a Poiseuille-type flow, starting from $0.1\, u_{*1} y_{01}$ near the high-stress wall ($y/y_{01} = 0.5$) and ending at $0.1\, u_{*2} y_{02}$ near the low-stress wall ($y/y_{02} = 0.5$). In the wall layers themselves the mixing-length results (10) can be used to determine the diffusivity.

6. CONCLUDING REMARKS

The following empirical information relating to possibly asymmetric channel flows has been presented:

(a) friction laws expressing the pressure gradient and stresses at the two walls in terms of the volume flow through the channel and the relative velocity of the two walls;

(b) definition of the regions near the walls in which a conventional mixing-length formula is applicable;

(c) methods of estimating the eddy viscosity (or eddy viscosity distribution) in the core between the two wall layers;

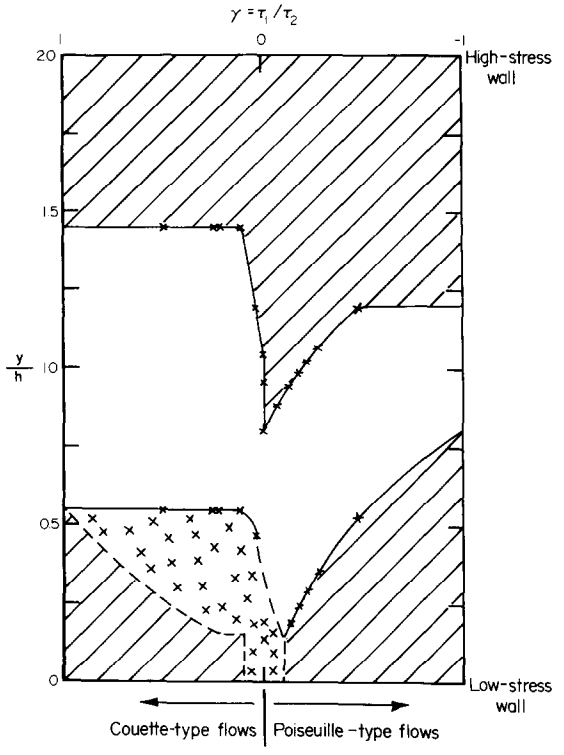

FIG. 11. Boundaries between regions where simple empirical models are applicable. See text for explanation.

(d) the failure of simple correlations near the low-stress wall in flows where $|\gamma| = |\tau_2/\tau_1| < 0.1$, that is, when the stress there is less than 10% of that at the other wall.

For clarity, the regions referred to in (b)–(d) are shown in Fig. 11. Shown hatched are regions in which the 'standard' mixing-length description of the wall layer is applicable (immediately adjacent to the wall the mixing length will be 'damped' by the increasing influence of viscosity). The extent of the core between the wall layers is indicated by the unhatched area of Fig. 11. Finally, near the low-stress wall there is a region (marked with crosses) where the velocity variation cannot be defined by one of the usual semi-empirical formulae. Some features of the flow in this region have been described elsewhere [1]. It is from this source that the region of applicability of the logarithmic velocity variation was derived. Moreover, it has been shown that the flow in the region marked with crosses can often be described as a 'gradient' or 'half-power' layer, where $U = C(\alpha y)^{1/2} + E$, with α the gradient of kinematic shear stress introduced in equation (7). Since the empirical constants C and E vary from flow to flow, we shall not attempt to define this layer more precisely here.

REFERENCES

1. M. M. M. El Telbany and A. J. Reynolds, Velocity distributions in plane turbulent channel flows, *J. Fluid Mech.* **100**, 1–29 (1980).
2. M. M. M. El Telbany and A. J. Reynolds, Turbulence in plane channel flows, *J. Fluid Mech.* **111**, 283–318 (1981).
3. M. M. M. El Telbany and A. J. Reynolds, The structure of plane Couette flow, submitted to *J. Fluids Engng Trans. ASME.*
4. A. J. Reynolds and M. M. M. El Telbany, Mean velocity and eddy viscosity in a buffer region, submitted to *J. Fluid Mech.*
5. K. Hanjalić and B. E. Launder, Fully developed asymmetric flow in a plane channel, *J. Fluid Mech.* **51**, 301–335, (1972).
6. D. Riabouchinsky, Etude expérimentale sur le frottement de l'air, *Bull. Inst. Aérodynamique Koutchino,* **V**, 51–72 (1914).
7. J. Laufer, The structure of turbulence in fully developed pipe flow, NACA, Report 1174 (1954).
8. A. K. M. F. Hussain and W. C. Reynolds, Measurements in fully developed turbulent channel flow, *J. Fluids Engng Trans ASME* **97**, 568–578 (1975).

APPENDIX

SHEAR STRESS MEASUREMENTS

The turbulent shear stress was measured with a DISA X-wire probe (Type 55P61) in conjunction with two DISA 55M system constant-temperature anemometers, two 55M25 linearizers, a 55D35 r.m.s. voltmeter and a Datron 1045 digital voltmeter.

The probes were calibrated in pure pressure flow through the test channel itself. The wall-stress values used in reducing our measurements were obtained by extrapolation of the linear variations of Reynolds stress obtained using the X-wire probe This way of determining the wall stress was checked in pure pressure flow by comparison with the streamwise pressure gradient and in the wider class of flows by the coalescence of the several sets of results on the line $U/u_* = yu_*/\nu$.

DESCRIPTION EMPIRIQUE DES ECOULEMENTS TURBULENTS EN CANAL

Résumé—On présente sous la forme de longueurs de mélange et de viscosités turbulentes des mesures faites sur 26 écoulements turbulents disymétriques (c'est à dire écoulements dans un canal large avec des contraintes inégales sur les deux parois). Les domaines de validité des formules empiriques simples sont définis et des lois de frottement pour les contraintes pariétales sont données.

DIE EMPIRISCHE BESCHREIBUNG TURBULENTER KANALSTRÖMUNGEN

Zusammenfassung—Messungen in sechsundzwanzig asymmetrischen turbulenten Kanalströmungen (d.h. Strömungen in einem breiten Kanal, insbesondere mit ungleichen Wandschubspannungen an beiden Wänden) werden in der Form von Mischungsweglänge und turbulenter Zähigkeit wiedergegeben.

Die Gültigkeitsbereiche einfacher empirischer Formeln werden definiert und Reibungsgesetze für die Wandschubspannungen entwickelt.

ЭМПИРИЧЕСКОЕ ОПИСАНИЕ ТУРБУЛЕНТНЫХ ТЕЧЕНИЙ В КАНАЛАХ

Аннотация — Измерения, проведенные в двадцати шести асимметричных турбулентных течениях в каналах (а именно в широком канале с неодинаковыми напряжениями на обеих стенках) представлены в виде выражений для длин смешения и вихревой вязкости. Определены области применимости простых эмпирических формул и предложены законы трения для напряжений на стенке.